Received: 23 August 2018 | Revised: 4 January 2019 | Accepted: 7 January 2019

DOI: 10.1002/aoc.4838



FULL PAPER

WILEY Applied Organometallic Chemistry

# Selective functionalization of ferrocenyl compounds using a novel solvent free synthetic method for the preparation of bioactive unsymmetrical ferrocenyl derivatives

Avishek Ghosh[1] | Tulasi Barik[1] | Smriti Dewangan[1] | Paresh Kumar Majhi[2] | Takahiro Sasamori[2] | Shaikh M. Mobin[3] | Santanab Giri[4] | Saurav Chatterjee[1]

[1]Department of Chemistry, National Institute of Technology Rourkela, Rourkela 769008, India

[2]Graduate School of Natural Sciences, Nagoya City University, Nagoya, Aichi 467-8501, Japan

[3]Schools of Basic Science, Indian Institute of Technology Indore, MP 452017, India

[4]Theoretical Chemistry Laboratory, Department of Chemistry, National Institute of Technology Rourkela, Rourkela 769008, India

**Correspondence**
Saurav Chatterjee, Department of Chemistry, National Institute of Technology Rourkela, Rourkela 769008, India.
Email: saurav@nitrkl.ac.in

**Present Address**
Santanab Giri, Department of Applied Sciences, Haldia Institute of Technology, ICARE Complex, Haldia-721657, W.B, India.

**Funding information**
Science and Engineering Research Board, Department of Science and Technology, India, Grant/Award Number: SB/S1/IC-30/2013

A novel solvent free synthetic method has been designed by using rice husk ash (RHA) as solid support for the selective functionalization of ferrocenyl derivatives and described the synthesis of a 1,1′-unsymmetrically bi-functionalized ferrocenyl compounds for their biological evaluation. Single crystal X-ray structural evaluation showed some interesting intra-molecular hydrogen bonding interactions across the chains of the ferrocenyl molecule, while DFT calculation revealed the significance of the orientation between the two cyclopentadienyl rings for the hydrogen bonding interaction. Redox and antibacterial properties have been studied to understand the electronic and biological effect of different hydrazone system and their potential for future application.

**KEYWORDS**
antibacterial, ferrocenyl, selective substitution, solvent free

## 1 | INTRODUCTION

Use of inorganic support in chemical synthesis has attracted much attention due to their ability to perform reactions under mild conditions, easy product isolation procedures and higher yield.[1,2] Solid state, solvent free reactions using organic substrates are widely used for improved product synthesis, while solid supported reactions involving organometallic fragments have been rarely studied.[3] During the last decade, functionalization of ferrocene with biologically active moieties and their study on different bioactivity have led to the immergence of a new field of bio-organometallic chemistry.[4] Investigation on ferrocene substituted tamoxifen and ferrocenyl

  

chloroquine derivatives are among the many examples where systematic functionalization of ferrocene have improved the activity of the drug.[4h–k] Replacement of aromatic groups with ferrocenyl moieties in penicillin and cephalosporine and introduction of various ferrocene based chains reportedly enhances the antibacterial potency of therapeutic drugs.[4l-r] Moreover, the emergence of bacterial resistance to commercial antibiotics has compelled us to search for new class of antimicrobial compounds with different mode of action to curb the problem of multi-resistant pathogens. Recently, ferrocene based organometallic molecular entities have proved their ability by showing inhibitory activities towards several microbes.[4] We have also focused our study on the biological aspects of various ferrocene based molecular systems ranging from ferrocenyl hydrazones, hetero-bimetallic ferrocenyl chalcones, ferrocene based cluster compounds, ferrocenyl dithiocarboxylates and multi-ferrocenyl compounds and reported their significant biological properties.[5] Recently, bi-functionalization of ferrocene in the form of 1,1′-unsymmetrically di-substituted derivatives (Figure 1, Type C) have shown remarkable sensor based, biological and catalytic properties.[5a,6] However, selective synthesis of these unsymmetrically disubstituted ferrocenyl derivatives has been a challenge due to the formation of symmetrical di-substituted product (Type A) in major amount, resulting in either very low yield or non formation of the required unsymmetrical derivative of the type B. As a result, ferrocenyl compounds containing unsymmetrical substitution (Type C) are far less known than their symmetrical analogue. Nevertheless, we could able to isolate 1,1′- unsymmetrically bi-functionalized ferrocenyl compounds (Type C) involving a two step solution based reaction process,[5a] and observed interesting sensing and

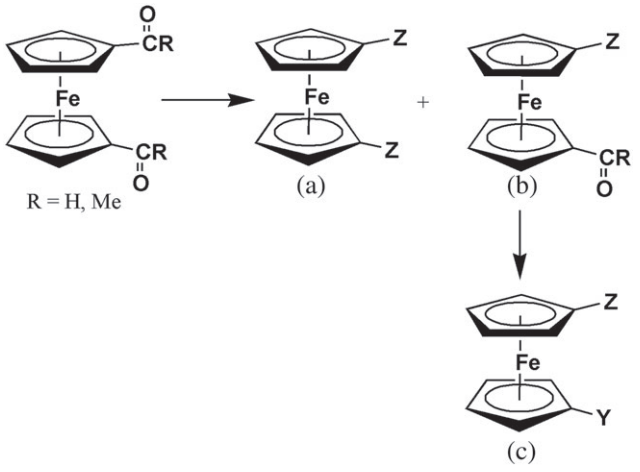


**FIGURE 1** Type A: Symmetrical substitution, Type B: Unsymmetrical substitution, Type C: Bi-functional unsymmetrical substitution

electro-communication properties, but the overall yield of the compounds has been significantly less for any practical application. The low yield has been mainly due to the non-selective reaction process resulting in reduced formation of the unsymmetrical product (Type B). Therefore, we continued our investigation to find an ideal system where one of the cyclopentadienyl (Cp) rings of a ferrocenyl fragment can be selectively substituted with respect to the other ring. A range of different bi-functionalized unsymmetrical compounds can be prepared once the first substitution is achieved selectively, followed by an easier second substitution at the pendant Cp ring. Such selective substitution has been a challenge for system like diacetyl- and dialdehyde ferrocene which are widely used as precursor for a variety of ferrocene based functional products.[7] This prompted us to investigate a process involving solid state synthetic method for the selective substitution of Cp rings in diacetyl and dialdehyde ferrocene compounds and understand their potential for the synthesis of bi-functional molecules.

In our study we have chosen Rice husk ash (RHA) as solid support due its high silica content, wide availability and to understand its usage in synthetic reactions. RHA is obtained when rice husk is burnt during their use as fuel in the rice mills and left unused.[8] Efforts are going on in global research to use this RHA in several fronts.[9] To the best of our knowledge Rice Husk Ash (RHA) has never been studied extensively for their role to support/mediate chemical reactions. In this report, we describe the use of RHA in supported condensation reactions for selective functionalization of diacetyl and dialdehyde ferrocenyl compounds and report the synthesis of novel bifuntionalized unsymmetrical ferrocenyl derivative and their high antibacterial activity. Structural characterization of the two unsymmetrically substituted ferrocenyl compounds have been carried out and their hydrogen bonding features and conformational orientations were investigated. Cyclic voltammetric studies and DFT calculation have also been reported to understand their redox system, bonding features and future application.

## 2 | RESULTS AND DISCUSSION

Reaction of 1,1′-diacetylferrocene (135 mg, 0.5 mmol) with respective hydrazides (0.5 mmol) in presence of rice husk ash (RHA, 1gm) as solid support gave selectively single mono-functionalized products, 1,1′-[$CH_3C(O)(\eta^5$-$C_5H_4)Fe\{(\eta^5$-$C_5H_4)C(CH_3)$═N-N(H)C(O)-R}] {R = $C_6H_5$ (**1a**), $C_6H_4$-OH (**1b**), $CH_2CN$ (**2**)} in high yield with exceptional selectivity (Scheme 1). Table 1 shows the selectivity for the formation of mono- functionalized product with increasing amount of hydrazide ratio up to 5 equivalents.

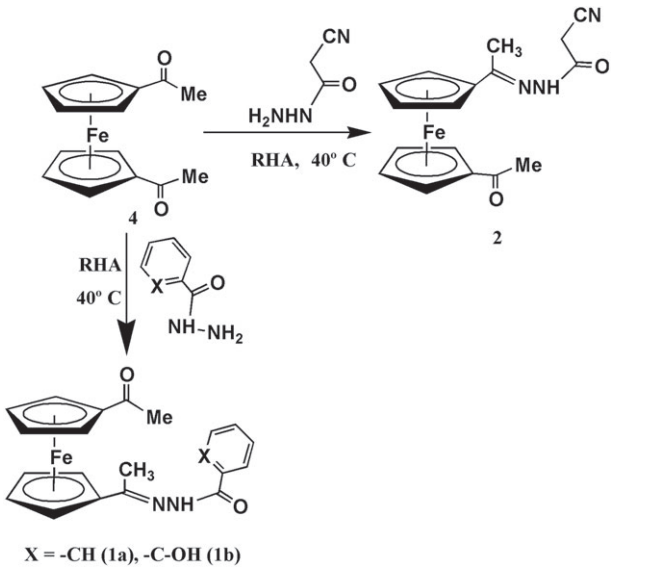


**SCHEME 1** Synthesis of **1a**, **1b** and **2**

In our earlier report, we observed the formation of **1a** and **1b** in much lower yields along with a major amount of symmetrically di-substituted ferrocenyl compound by solution based method in weakly acidic condition.[5a] The mono-functionalized compound of the type A are the key precursor for the synthesis of 1,1′- unsymmetrically bi-functionalized ferrocenyl compounds (Type C) which have interesting sensing and electro-communication properties.[5a,6] However, the use of rice husk ash (RHA) as solid support gave highly selective substitution at one of the cyclopentadienyl ring of the ferrocenyl system to obtain compounds **1a**, **1b** and **2**. To understand the selectivity of the reaction obtained under RHA condition, we investigated the surface properties of the RHA using BET and FESEM techniques. BET surface analysis reveals a pore size diameter of around 40 Å (Figure S26) and an average surface area of 126 $m^2/g$. The mesoporous nature of the particles has also been revealed by the BET adsorption isotherm analysis (Figure S27). The FESEM image shows the presence of nanosized particles in the range 30–60 nm with highly porous surface morphology (Figure S25). The remarkable surface properties of RHA with high porosity, nanosize particles and acidic nature of silica may have been responsible for the selective interaction of the substrate giving rise to selective functionalization. Compounds **1a** and **1b** were isolated and their spectral data was compared with the previously reported data,[5a] while **2,** as per our knowledge**,** is a newly synthesized compound and has been characterized by IR, NMR and Mass spectroscopy. Infrared spectrum of **2** shows the presence of -C≡N and keto groups at 2246 $cm^{-1}$ and 1696 $cm^{-1}$, 1668 $cm^{-1}$ regions respectively, while -C═N vibration peak has been observed at 1622 $cm^{-1}$. $^1H$ NMR spectral analysis shows two methyl peaks at δ 2.14 and δ 2.37 and one peak at δ 3.84 corresponding to methylene proton. Peaks for ferrocenyl protons have been observed between δ 4.43 – δ 4.79 region while a peak at δ 8.59 has been attributed to NH group present in the molecule. $^{13}C$ NMR spectral analysis reveals the presence of peaks at δ 14.35, δ 24.73 and δ 27.69 region corresponding to methyl and methylene carbon, while cyclopentadienyl carbon peaks has been found between δ 84.04 - δ 68.62 region. The spectrum also shows peaks in the downfield region at δ 114.38, δ 151.19, δ 164.64 and δ 201.65 regions which may corresponds to –C=N, -C=O and -C≡N groups respectively. Mass spectral analysis of compound **2** shows the presence of $[M + 1]^+$ peak at m/z 352.8.

**TABLE 1** Selectivity and yields for the formation **1a**, **1b** and **2**

| $[Fe\{(\eta^5\text{-}C_5H_4)(COCH_3)\}_2]$ | $[H_2NNC(O)R]$ R = $C_6H_5$, $C_6H_4OH$, $CH_2CN$ | Reaction condition | Yields-Mono-functionalized Product | Yields-Di-functionalized Product (Type A) | Selectivity |
|---|---|---|---|---|---|
| 0.5 mmol (135 mg) | 0.5 mmol | 6 hrs., 50 °C | 186 mg (**1a**)<br>194 mg (**1b**)<br>172 mg (**2**) | Negligible<br>Negligible<br>nil | ~99% (**1a**)<br>~99% (**1b**)<br>~100% (**2**) |
| 0.5 mmol(135 mg) | 1 mmol | 6 hrs., 50 °C | 182 mg (**1a**)<br>190 mg (**1b**)<br>173 mg (**2**) | Negligible<br>Negligible<br>nil | ~99%(**1a**)<br>~99% (**1b**)<br>~100% (**2**) |
| 0.5 mmol (135 mg) | 1.5 mmol | 6 hrs., 50 °C | 180 mg (**1a**)<br>186 mg (**1b**)<br>168 mg (**2**) | 10 mg<br>12 mg<br>Negligible | ~96% (**1a**)<br>~95% (**1b**)<br>~98% (**2**) |
| 0.5 mmol (135 mg) | 2 mmol | 6 hrs., 50 °C | 177 mg (**1a**)<br>185 mg (**1b**)<br>166 mg (**2**) | 12 mg<br>13 mg<br>Negligible | ~95% (**1a**)<br>~95% (**1b**)<br>~98% (**2**) |

N.B.: The yields of the product have been calculated on the basis of the amount of reactant consumed.

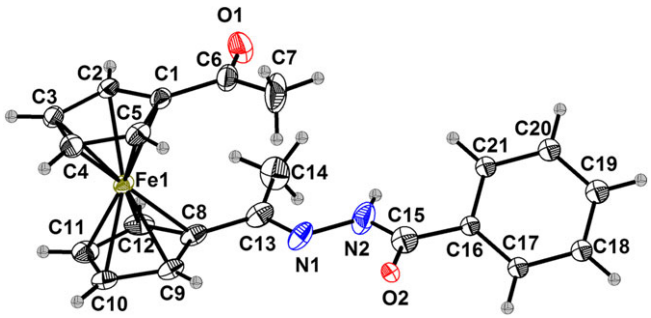


**FIGURE 2** Molecular structure of **1a.** Selected bond lengths (Å) and bond angles (°): N(1)-C(13) = 1.297(6), N(1)-N(2) = 1.390(6), O(2)-C(15) = 1.231(12), O(1)-C(6) = 1.220(7), Fe(1) – C(1) = 2.051(4), N(1)-N(2)-C(15) = 113.66(1), C(13)-N(1)-N(2) = 115.46(0), C(1)-C(6)-C(7) = 117.24(1)

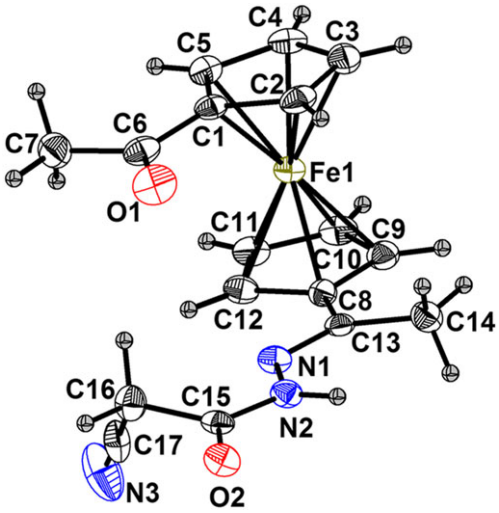


**FIGURE 4** Molecular structure of **2.** Selected bond lengths (Å) and bond angles (°): N(1)-C(13) = 1.291(1), N(1)-N(2) = 1.387(0), O(2)-C(15) = 1.238(0), O(1)-C(6) = 1.216(0), N(3)-C(17) = 1.141(0), Fe(1) – C(1) = 2.038(4), N(1)-N(2)-C(15) = 117.9(0), C(13)-N(1)-N(2) = 117.65(0), C(1)-C(6)-C(7) = 117.12(0), C(16)-C(17)-N(3) = 117.21(0)

Molecular structure of **1a** confirms the presence of a $-COCH_3$ group attached to one of the cyclopentadienyl ring of the ferrocenyl fragment, while the other ring is linked to a hydrazone unit via a -C═N bond (Figure 2). The structural analysis confirms a double bond character of C(13)-N(1) bond with a bond length of 1.297(6) Å, while N(1)-N(2) corresponds to single bond character (1.390(6) Å). The two ferrocenyl cyclopentadienyl rings are oriented in eclipsed conformation with a dihedral angle of 0.6° between the two substitutions at C1 and C8 position. The plane of the phenyl ring is perpendicular to the Cp ring in contrast to the earlier structure of the pyridyl derivative, 1,1′-[$CH_3C(O)(\eta^5\text{-}C_5H_4)Fe\{(\eta^5\text{-}C_5H_4)C(CH_3)$═$NN(H)C(O)(C_5H_4N)\}$].[5a] The C-O bond length corresponding to the ketonic group of the hydrazone chain is slightly longer (C(15)-O(2) = 1.231(12) Å) than the ketonic group linked to the other Cp ring (C(6)-O(1) = 1.220(7) Å). Packing diagram reveals three inter-molecular hydrogen bonding interactions between O2 ... H-C7, O2 ... H-N2 and O2 ... H-C14 with the formation of a linear polymeric chain with alternate molecular units (Figure 3).

Molecular structure of **2** confirms the structural integrity with the presence of a ferrocenyl moiety attached to an acetyl group at one of the cyclopentadienyl ring and a hydrazone chain of the type $-C(CH)_3NN(H)C(O)CH_2CN$ at the other ring as shown in Figure 4. The hydrazone chain contains an active methylene group in contrast to aromatic group present in compound **1a**. The molecule shows both inter- and intra-molecular hydrogen bonding as shown in Figure 5. The intra-molecular hydrogen bonding has been observed between the $CH_2$ proton of the hydrazone chain and the oxygen atom of the acetyl group attached to the other Cp ring of the same ferrocenyl moiety. The presence

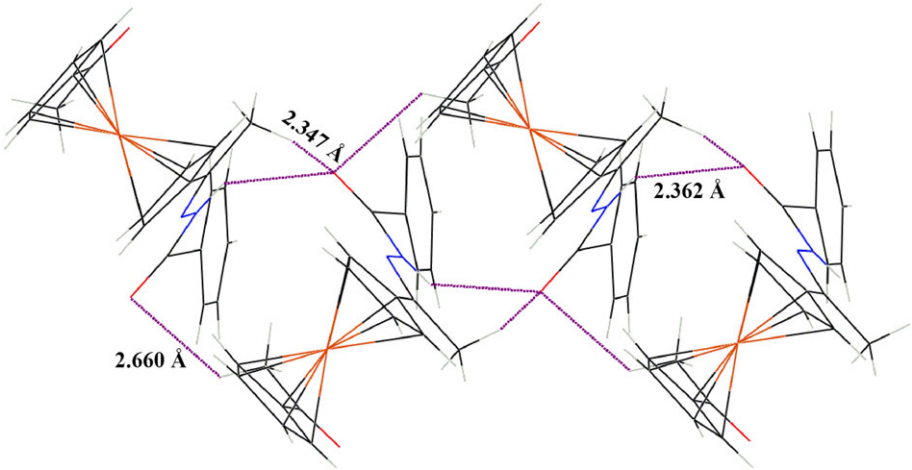


**FIGURE 3** Inter-molecular Hydrogen-bonding interactions in **1a**

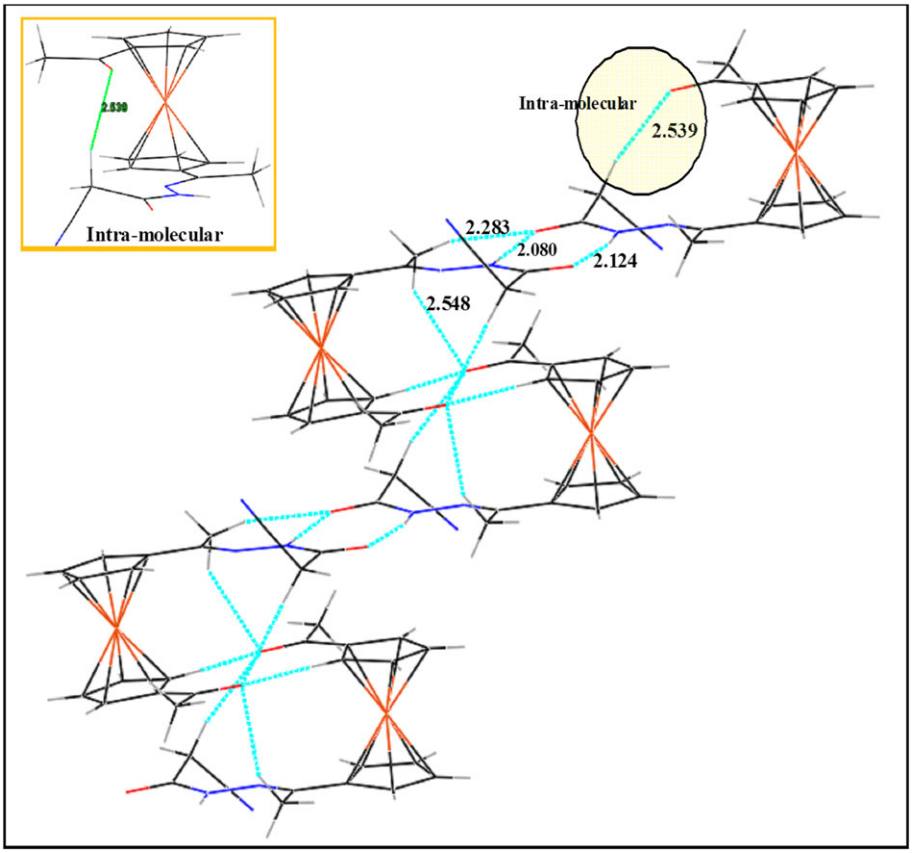


**FIGURE 5** Hydrogen bonding interactions in **2**

of intra-molecular hydrogen bonding interaction across the two side chains of the Cp rings may have been responsible for the formation of a non-eclipsed type orientation of the Cp rings with a torsional angle of 59.6°. The staggered conformational feature of **2** is new in contrast to **1a** and some earlier reported similar type of mono-functionalized compounds with eclipsed conformation.[5a] Across the chain hydrogen bonding interactions has been well established in some significant ferrocene - peptide conjugates for their analogy with several biomolecular system. To establish the basis of the hydrogen bonding interaction across the chains in compound **2**, DFT calculation was carried out, the results of which has been depicted later.

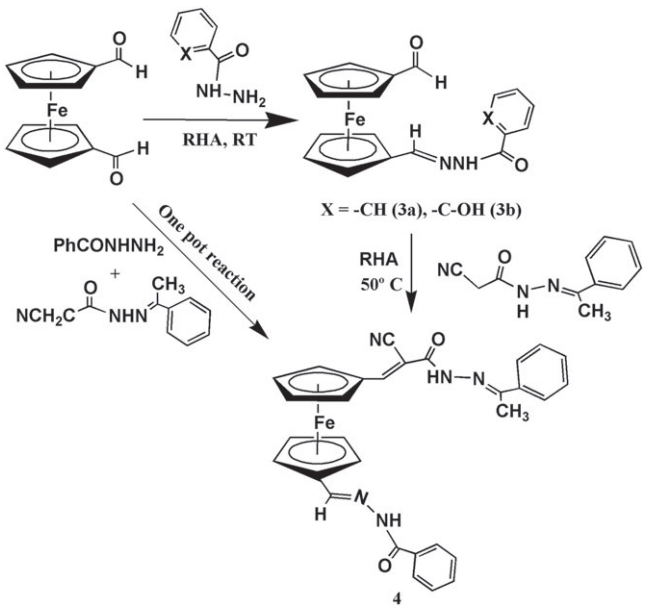


**SCHEME 2** Synthesis of **3a**, **3b** and **4**

In another solvent free reaction of 1,1′-ferrocenylcarboxyaldehyde with the respective hydrazides involving Rice husk ash (RHA) as solid support gave selectively mono-substituted product, 1,1′-[CH(O)($\eta^5$-$C_5H_4$)Fe{($\eta^5$-$C_5H_4$)C(H) = NN(H)C(O)R}] {R = $C_6H_5$ (**3a**), $C_6H_4$-OH (**3b**)} in high yields (Scheme 2). Compounds **3a, 3b** were characterized using IR, NMR and mass spectroscopic techniques. Infrared spectra for compounds **3a, 3b** show peaks corresponding to C=O and C=N stretching frequency in the range 1681–1607 $cm^{-1}$ region. $^1$H NMR spectra of **3a** and **3b** reveals the presence of four triplet (or broad) peaks at δ 4.48–4.89 region corresponding to eight substituted ferrocenyl Cp protons and a multiplet at δ 6.92–8.09 region for phenyl protons in each of the two compounds. One singlet peak at δ 9.94 region has been observed for both **3a** and **3b** due to

the presence of aldehyde proton. A singlet peak at downfield region (δ 11.92) shows the presence of -OH proton in compound **3b**. NH protons have also been observed at δ 9.27 and δ 9.55 for compounds **3a** and **3b** respectively. Mass spectral analysis of compounds **3a** shows the presence of $[M + 1]^+$ peak at m/z 362.

Further reaction of **3a** with acetophenone 2-cyanoacetohydrazone (**5**) under solvent free condition using RHA as solid support gave a bi-functionalized unsymmetrically substituted compound **4** in substantial yield as shown in Scheme 2. This shows that the solid RHA also catalyzes Knoevenagel type condensation reaction between an aldehyde group and active methylene unit. Effort to undergo a multi-component reaction in one pot condition using ferrocenyl dialdehyde, benzoic hydrazide and **5**, also gave compound **4** without the need for isolation of **3a**. Compound **4** was characterized by IR, NMR and Mass spectrometry. The infrared spectral data for **4** show bands corresponding to C≡N, ketonic and C=N units at 2210 $cm^{-1}$, 1651 $cm^{-1}$, and 1606 $cm^{-1}$ regions respectively. $^1$H NMR spectra reveals the presence of $CH_3$ protons at δ 2.31 and substituted ferrocenyl Cp peaks at δ 4.44, δ 4.79, δ 4.94, δ 5.13 regions, while peaks for phenyl protons have been observed at δ 7.40–8.06 (multiplet) region. Two singlet peaks corresponding to olefinic protons have been observed at δ 7.76 and δ 8.16 regions and -NH protons have also been observed at δ 9.26 and δ 9.78 region. Mass spectral analysis showed $[M + 1]^+$ peak at m/z 544 region. Formation of compound **4** revealed that RHA can also be used as support for Knoevenagel condensation. Attempts to prepare **4** using different solution based method were not successful. Therefore, we directed our study on the selectivity of Knoevenagel based condensation reactions involving ferrocenyl dialdehyde and an active methylene substrate using rice husk ash as support.

Solvent free solid supported reaction of ferrocenyl dialdehyde with acetophenone 2-cyanoacetohydrazone (**5**) or 1-(coumarin-3-yl)ethylidene 2-cyanoacetohydrazone (**6**) using RHA gave selectively unsymmetrically mono-substituted product (**7**, **8**) (Scheme 3). To the best of our knowledge, this is a first report on the selectivity of Knoevenagel type condensation on ferrocenyl system. In comparison, solution based Knoevenagel condensation of ferrocenyl dialdehyde with **5** or **6** using piperidine gave di-substituted product in major amount. Both the compounds, **5** and **6** have been prepared using a modified procedure involving RHA as solid support and characterized using IR and NMR spectroscopic technique. The spectra were matched with that in the previously reported literature.[10] The unsymmetrically mono-functionalized compounds, **7** and **8**, was also obtained by a solid state one pot reaction condition using acetophenone or acetyl coumarin, 2-cyanoacetohydrazide, ferrocenyl dialdehyde and RHA. Characterization of compounds **7** and **8** with IR, NMR and mass spectroscopic technique confirmed their structural features. Infrared spectra for both **7** and **8** showed bands at 2214 $cm^{-1}$ due to the presence of C≡N group and at 1730–1663 $cm^{-1}$ region for the presence of ketonic groups. $^1$H NMR spectral analysis for **7** and **8** show methyl peaks at δ 2.42 and δ 2.43 region respectively and peak for olefinic proton has been observed at δ 8.24 - δ 8.27 region. Ferrocene based cyclopentadienyl protons have been observed between δ 4.68 – δ 5.11 region while peaks at δ 7.32 – δ 8.25 (multiplet) corresponds to aromatic protons for phenyl and coumarin moieties. A singlet peak at δ 9.91 and δ 9.89 has been observed for **7** and **8** respectively due to the presence of aldehyde proton and peaks at δ 9.26 and δ 9.36 shows the presence of -NH proton for compounds **7** and **8** respectively. Mass spectral analysis of compound **8** shows the presence of $[M + 1]^+$ peak at m/z 494.

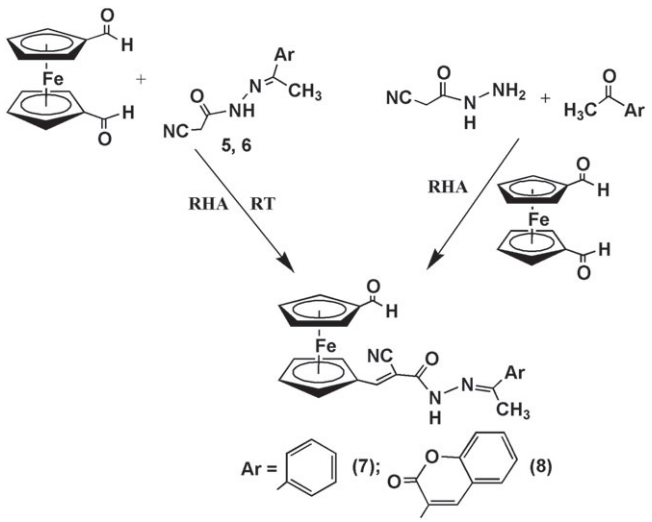


**SCHEME 3** Synthesis of **7** and **8**

## 2.1 | Redox properties study

The electrochemical properties of compounds **2, 3a, 3b, 4, 7** and **8** were examined in acetonitrile solution (0.1 M TBAP) by cyclic voltammetry (CV) and differential pulse voltammetry. Compound **2**, involving a ferrocenyl moiety and linked to one cyanoacetohydrazide group exhibited a reversible redox process at +0.66 V ($E_{1/2}$) due to the Fe (II)/Fe (III) redox couple which is slightly lower than the redox peak observed for compound **1a** ($E_{1/2}$ = 0.69 V), while the potential value is similar to that of compound **1b** ($E_{1/2}$ = 0.66 V) (Figure 6).[5a] Both the compounds **3a** and **3b** showed the corresponding

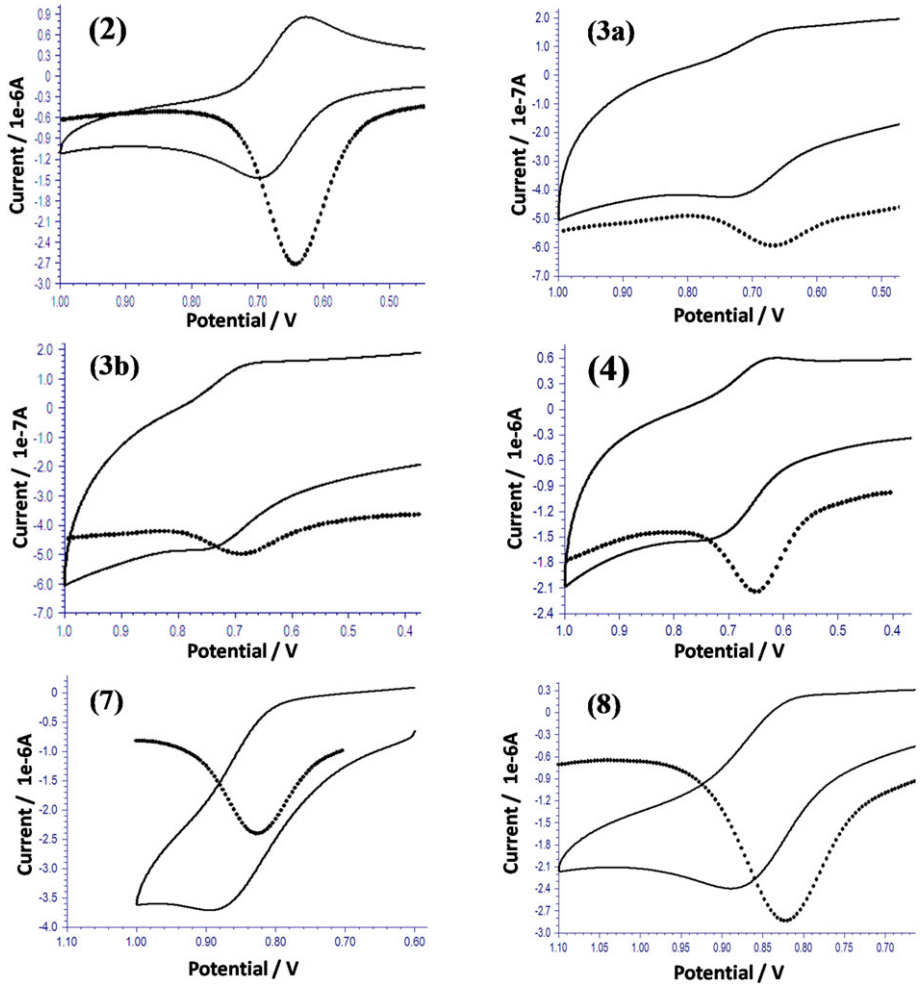


**FIGURE 6** Cyclic voltammograms (—) and differential pulse voltammograms (...) of compounds **2**, **3a**, **3b**, **4**, **7** and **8** in Acetonitrile/0.1 M TBAP at 298 K

**TABLE 2** Cyclic voltammetric data

| Compounds | $Ep_a$ (V) | $Ep_c$ (V) | $E_{1/2}$ (V) ($\Delta E$ (mV)) | dpv (V) | Ref. |
|---|---|---|---|---|---|
| **1a** | 0.717 | 0.657 | 0.69 (60) | 0.66 | [5a] |
| **1b** | 0.69 | 0.633 | 0.66 (57) | 0.634 | [5a] |
| **2** | 0.695 | 0.633 | 0.664 (62) | 0.642 | - |
| **3a** | 0.72 | 0.676 | 0.698 (44) | 0.67 | - |
| **3b** | 0.72 | 0.68 | 0.7 (40) | 0.687 | - |
| **4** | 0.72 | 0.65 | 0.685 (70) | 0.65 | - |
| **7** | 0.88 | 0.81 | 0.845 (70) | 0.83 | - |
| **8** | 0.88 | 0.83 | 0.85 (50) | 0.82 | - |
| **Fc $(CHO)_2$** | 0.89 | 0.82 | 0.855 (70) | 0.83 | [10] |

In acetonitrile at a scan rate of 50 mv $s^{-1}$. $E_{1/2}$ (V) = $(E_{pa} + E_{pc})/2$, where $E_{pa}$ and $E_{pc}$ are the anodic and cathodic peak potentials respectively. $\Delta E_p$ (mV) = $E_{pa}$-$E_{pc}$.

Fe (II)/Fe (III) redox couple at higher potential ($E_{1/2}$ = +0.7 V) due to the presence of an aldehyde group at one of the cyclopentadienyl ring of the ferrocenyl fragment (Table 2). However, functionalization of a Cp ring with acetophenone cyanoacetohydrazone in **7** exhibited a much higher redox couple at +0.845 V, which shows a better electron withdrawing property of the hydrazone chain and the presence of a donor-acceptor type of system in the molecule. Compound **8** with a coumarin fragment attached to the hydrazone chain also shows a redox couple at the oxidative potential of +0.85 V. However, The potential value of both **7** and 8, are slightly lower than the redox couple of Fe (II)/Fe (III) in dialdehyde ferrocene ($E_{1/2}$ = +0.855 V). The bifunctionalized unsymmetrical compound **4**, exhibited a reversible redox process at +0.685 V ($E_{1/2}$) due to the Fe (II)/Fe (III) couple which is higher than that in **1** and **2** but lower than **3**, **7** and **8** (Table 2). This reveals that the electron withdrawing behaviour of the hydrazone chain is lower than that of a cyanovinyl linkage, which have similar electron withdrawing tendency as a –CHO group.

## 2.2 | DFT study

DFT calculation was carried out with fully optimized geometry of compound **2** in gas and solution phase for different orientation of ferrocenyl system using B3LYP and M06-2X functionals. Energy calculation was carried out with the optimized geometry of three different orientations of compound **2**: One with the geometry of the X-ray crystal data having a torsional angle (θ) between the two Cp rings of 59.6°, another with eclipsed geometry (torsional angle θ = 0°) and an additional with the fully staggered geometrical orientation having a torsional angle (θ) of 144°. The single crystal structure of compound **2** with non -eclipsed conformation shows intra- molecular hydrogen bonding in –between the two side chains of the same ferrocenyl moiety. This type of intra-molecular H-bonding has not been observed with analogous compounds, **1a** and **1b**. This prompted us to look into the details of the basis of the hydrogen bonding interaction across the side chains. Hydrogen bonding interactions play a vital role in several biomolecules and have been observed recently in some disubstituted ferrocenyl-peptide molecular system.[11] These ferrocene based peptide molecule also shows intra - molecular hydrogen bonding interactions across the peptide side chain, comparable to that in biomolecules. In our study, we anticipated that the H-bonding interaction across the side chain in compound **2** was due to a specific orientation of the two Cp rings. To understand the details of the interaction we carried out energy calculation with the optimized geometry of three different orientations of compound **2**: One with the geometry of the X-ray crystal data having a torsional angle (θ) between the two Cp rings of 59.6°, another with eclipsed geometry (torsional angle θ = 0°) and an additional with the geometrical orientation having a torsional angle (θ) of 144°. Figure 7 depicts the DFT optimized structure of different orientation having θ = 0°, 59.6° and 144° respectively. Gas phase calculation using M06-2X functional shows that the energy for the orientation with θ = 59.6° is 0.18 eV more stable than the fully staggered geometry with higher torsional angle of 144°, but slightly less stable (0.032 eV) than that for the eclipsed orientation. Solution phase calculation with dichloromethane and ethanol solvents also showed similar energy behavior. Calculation using both B3LYP and M06-2X functional reveals the presence of intramolecular hydrogen bonding interaction between the ketonic oxygen and methylene hydrogen group across the two Cp rings for θ = 59.6° orientation in gas phase as well as in solution phase. The hydrogen bond distances, calculated in gas phase is always shorter (2.04 Å) than that calculated in dichloromethane and ethanol solvent phases (2.072, 2.089 Å). In contrast, the orientations with θ = 0°, and 144° does not show –CH...O=C- intramolecular hydrogen bonding interactions across the Cp rings. On the contrary, a different intramolecular hydrogen bonding interaction between the NH group of the hydrazone chain and ketonic oxygen of the other chain with a distance of 2.45 Å has been observed for the eclipsed conformation with θ = 0°. The hydrogen bonding distances and the energies for different orientations have been depicted in Table 3. Among the two solvents, energy calculation of ethanol solution in 0°, 59.6° and 144° orientation showed 0.075 eV, 0.082 eV and 0.012 eV more stable than that in dichloromethane phase respectively, probably due to the higher polarity of ethanol which may have increased the hydrogen bonding interactions with the solvent molecules (Table 3).

Molecular orbital diagram for **2** were generated to understand the involvement of different moieties and their possibility for any electronic conjugation within the hydrazone chain. Molecular orbital calculation for the three orientations (θ = 0°, 59.6°, 144°) shows that the Highest occupied molecular orbital (HOMO) of the ferrocenyl system with θ = 59.6° shows the involvement of metal d-orbitals and the hydrazone chain, while the LUMO is localized on the ketonic group of the pendant acetyl fragment (Table S1, S2).

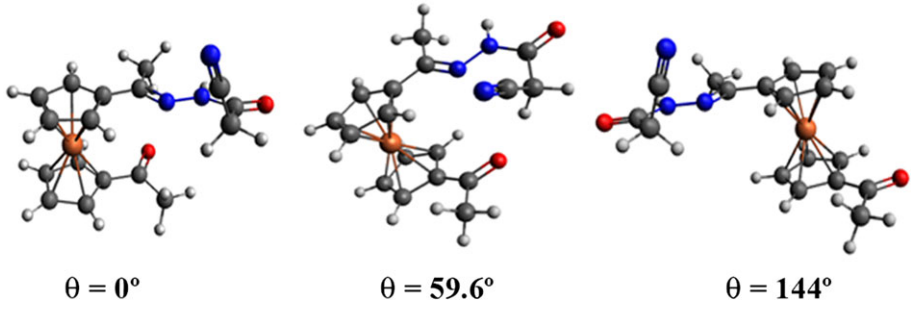


**FIGURE 7** Optimized structure of **2** with θ = 0°, 59.6° and 144°

**TABLE 3** Energy calculation of **2**

| 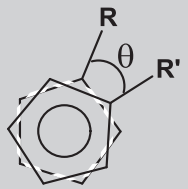 **2**: R = -$COCH_3$, R' = -$C(CH_3)NNHC(O)CH_2CN$ | Gas Phase Calculation (eV) | Solution Phase Calculation | | Intra-molecular H-bond Distance (C-H ... O-C-) |
|---|---|---|---|---|
| | | Ethanol (eV) | $CH_2Cl_2$ (eV) | |
| θ = 0° | −29814.84[a], −29803.21[b] | −29815.49[a] −29803.84[b] | −29815.41[a], −29803.77[b] | C-H ... O-C- type intra-molecular H-bonding not observed |
| θ = 59.6° | −29814.88[a] −29803.18[b] | −29815.52[a] −29803.82[b] | −29815.44[a] −29803.7366[b] | 2.123 Å[a], 2.040 Å [b] (in gas phase) 2.187 Å[a], 2.072 Å[b] (in $CH_2Cl_2$) 2.213 Å[a], 2.089 Å[b] (in EtOH) |
| θ = 144° | −29814.75[a], −29803.00[b] | −29815.50[a], −29803.72[b] | −29815.40[a] −29803.7367[b] | C-H ... O-C- type intra-molecular H-bonding not observed |

[a]Calculated using B3LYP functional,

[b]Calculated using M06-2X functional.

**TABLE 4** Minimum inhibitory concentration (MIC) value in μg/ml

| Compounds | B. subtilis | E. coli | P. aeruginosa | V. cholerae |
|---|---|---|---|---|
| **2** | NS | 3.9 | 1.9 | 3.9 |
| **3a** | NS | 3.9 | 1.9 | 3.9 |
| **3b** | NS | 3.9 | 1.9 | 3.9 |
| **4** | 15.6 | NS | 1.9 | NS |
| **7** | 7.8 | 1.9 | 1.9 | NS |
| **8** | 15.6 | 3.9 | 1.9 | 3.9 |
| Vancomycin | 31.3 | 31.3 | 31.3 | -- |
| Ampicillin | 15.6 | 15.6 | 7.8 | 1.9 |

NS: Inhibitory activity not shown

## 2.3 | Antibacterial activity

Antibacterial study was carried out for compounds **2**, **3a**, **3b**, **4**, **7** and **8** against Gram positive *B. subtilis* and Gram negative *E. coli, P. aeruginosa, V. cholerae* bacterial strains. All the compounds showed high inhibition activity against the bacterial strains as shown in Table 4. Compounds **2**, **3a** and **3b** containing a mono-functionalized ferrocenyl hydrazone chain shows very similar inhibition behavior against *E. coli, P. aeruginosa, V. cholerae* bacterial strains, while no inhibitory response was observed against *B. subtilis*. In contrast, compound **4** with bi-functionalized chains showed good inhibitory effect against *B. subtilis* and *P. aeruginosa* bacterial strains. Compound **8** with a coumarin moiety attached to a ferrocenyl cyanovinyl chain showed high antibacterial activity with lower MIC values against all the studied bacterial strains. Presence of a cyanovinyl chain with a phenyl substituent, in compound **7**, also showed lower MIC values against *B. subtilis, E. coli* and *P. aeruginosa*. Our earlier reports showed moderate antibacterial activity with ferrocenyl hydrazone and enone based compounds, but the inhibitory properties shown by the ferrocenyl bi-functionalized compound (**4**) and cyanovinyl based compounds (**7**, **8**) are significantly high revealing their potential as medicinal agent. Significant antibacterial activity for the reported organometallic compounds could possibly be due to the presence of functionalized ferrocene based fragment which are supposed to play a vital role in increasing the cell permeability and lipophilicity of the compounds. Factors like electron delocalization and blocking of metal binding sites of the enzyme of microorganism are also responsible for the high inhibition activity in these compounds.

In summary, we have used Rice Husk Ash supported, solvent-free synthetic strategy for the selective functionalization of diacetyl – and dialdehyde- ferrocene which has been further reacted to obtain 1,1′-unsymmetrically bifunctionalized ferrocenyl derivatives. The ferrocene based compounds showed reversible one electron oxidative redox processes in varied potential range depending upon the chain attached to the cyclopentadienyl rings of the ferrocene moiety. Single crystal X-ray study showed a unique intramolecular hydrogen bonding interaction across the functionalized Cp rings potentially due to a specific conformational orientation as supported by DFT calculation. Some of the functionalized compounds showed

high antibacterial activity and can be useful for their application as potential drug candidate. We are presently focusing our research on the Donor-Acceptor property of the bi-functionalized molecular system to understand their influence in biological moieties for their therapeutic use.

## 3 | EXPERIMENTAL SECTIONS

### 3.1 | General procedures

All reactions and manipulations were carried out under an inert atmosphere of dry, pre-purified argon using standard Schlenk line techniques. Solvents were purified, dried and distilled under argon atmosphere prior to use. Infrared spectra were recorded on a Perkin Elmer Spectrum 2 spectrometer as $CH_2Cl_2$ solution and NMR spectra on a 400 MHz Bruker spectrometer in $CDCl_3$. Elemental analyses were performed on a Vario El Cube analyzer. Mass spectra were obtained on a SQ-300 MS instrument operating in ESI mode. Cyclic voltammetric and differential pulse voltammetric measurements were carried out using a CH Instruments model 600D electrochemistry system. A platinum working electrode, a platinum wire auxiliary electrode and a silver/silver chloride reference electrode were used in a three-electrode configuration. The supporting electrolyte was 0.1 M $[NEt_4]ClO_4$ and the solute concentration was ~$10^{-3}$ M. The scan rate used was 50–200 mV $s^{-1}$. All electrochemical experiments were carried out under a nitrogen atmosphere and are uncorrected for junction potentials. TLC plates (20x20 cm, Silica gel 60 F254) were purchased from Merck. [Fe($\eta^5$-$C_5H_4COCH_3)_2$], [Fe($\eta^5$-$C_5H_4CHO)_2$], [$H_2NN(H)C(O)R$], (R = -$C_6H_4$-OH, $C_6H_4$N-p, $C_6H_5$, $C_6H_4$N-o, $CH_2CN$) were prepared following reported procedures.[12–14]

### 3.2 | Synthesis of 1,1′-[$CH_3C(O)(\eta^5$-$C_5H_4)$Fe{($\eta^5$-$C_5H_4)C(CH_3)$=NN(H)C(O)R}] {R = $C_6H_5$ (1a), $C_6H_4$-OH (1b), -$CH_2CN$ (2)}

In a two neck round bottomed flask 1 gm of powdered Rice Husk Ash (RHA) was taken. Dichloromethane solution of 1,1′-diacetylferrocene (0.5 mmol, 135 mg) and respective hydrazide (0.5 mmol) was added and the mixture was evaporated to dryness using vacuum to obtain a solid mixture. The reaction mixture was then stirred continuously at 50 °C for six hours. After the reaction, the solid mixture was extracted in dichloromethane solvent, filtered and dried in vacuum. The residue was then dissolved in dichloromethane and purified using a short column chromatography. Rapid elution with 15% ethylacetate:n-hexane solvent mixture afforded an orange colored compound, 1,1′-[$CH_3C(O)(\eta^5$-$C_5H_4)$Fe{($\eta^5$-$C_5H_4)C(CH_3)$=NN(H)C(O)R}] {R = $C_6H_5$ (**1a**), $C_6H_4$-OH (**1b**), -$CH_2CN$ (**2**)}. (Yields: **1a**: 186 mg (96%); **1b**: 194 mg (96%); **2**: 172 mg (98%)).

**1a:** Anal. calcd. (found): C, 64.97 (65.12); H, 5.19 (5.05); N, 7.22 (7.34). IR($\nu$, $cm^{-1}$,$CH_2Cl_2$): 1666 (vs), 1650 (vs, br), 1603 (m), 1581 (m). $^1$H NMR (δ, $CDCl_3$): 2.09 (s, 3H, $CH_3$), 2.29 (s, 3H, $CH_3$), 4.33 (t, 2H, $\eta^5$-$C_5H_4$), 4.44 (t, 2H, $\eta^5$-$C_5H_4$), 4.75 (t, 2H, $\eta^5$-$C_5H_4$), 4.80 (t, 2H, $\eta^5$-$C_5H_4$), 7.42–7.86 (m, 5H, -$C_6H_4$). MS (ESI): m/z 389 $(M + 1)^+$.

**1b**: Anal. calcd. (found): C, 62.40 (62.58); H, 4.99 (4.86); N, 6.93 (6.84). IR($\nu$, $cm^{-1}$,$CH_2Cl_2$): 3086 (br), 1665 (vs), 1643 (s), 1605 (m), 1552 (s, br). $^1$H NMR (δ, $CDCl_3$): 2.21 (s, 3H, $CH_3$), 2.38 (s, 3H, $CH_3$), 4.45 (t, 2H, $\eta^5$-$C_5H_4$), 4.54 (t, 2H, $\eta^5$-$C_5H_4$), 4.84 (t, 2H, $\eta^5$-$C_5H_4$), 4.87 (t, 2H, $\eta^5$-$C_5H_4$), 6.93–7.56 (m, 4H, -$C_6H_4$), 11.89 (s, 1H, O*H*). MS (ESI): m/z 405 $(M + 1)^+$.

**2:** Anal. calcd. (found): C, 58.14 (58.36); H, 4.88 (4.74); N, 11.97 (12.14). IR($\nu$, $cm^{-1}$,$CH_2Cl_2$): 2248 (m), 1694 (vs), 1668 (vs), 1621 (m), 1455 (m). $^1$H NMR (δ, $CDCl_3$): 2.07 (s, 3H, $CH_3$), 2.34 (s, 3H, $CH_3$), 3.80 (s, 2H, C$H_2$), 4.41 (t, 2H, $\eta^5$-$C_5H_4$), 4.50 (t, 2H, $\eta^5$-$C_5H_4$), 4.67 (t, 2H, $\eta^5$-$C_5H_4$), 4.77 (t, 2H, $\eta^5$-$C_5H_4$), 8.59 (s, 1H, -N*H*). $^{13}$C NMR (δ, $CDCl_3$): 14.35 (-*C*$H_3$), 24.73 (-*C*$H_3$), 27.69 (-*C*$H_2$), 68.62 ($\eta^5$-*C*$_5H_4$), 70.78 ($\eta^5$-*C*$_5H_4$), 71.78 ($\eta^5$-*C*$_5H_4$), 73.40 ($\eta^5$-*C*$_5H_4$), 80.19 ($\eta^5$-*C*$_5H_4$), 84.04 ($\eta^5$-*C*$_5H_4$), 114.38 (-*C*=N), 151.19 (-*C*O), 164.64 (-*C*O), 201.65 (-*C*N). MS (ESI): m/z 352.8 $(M + 1)^+$.

### 3.3 | Synthesis of 1,1′-[CH(O)($\eta^5$-$C_5H_4$) Fe{($\eta^5$-$C_5H_4$)C(H)=NN(H)C(O)R}] {R = $C_6H_5$ (3a), $C_6H_4$–OH (3b)}

In a two neck round bottomed flask 1 gm of powdered Rice Husk Ash (RHA) was taken and dichloromethane solution of 1,1′- ferrocenyl carboxyladehyde (0.5 mmol, 121 mg) and the respective hydrazide (0.5 mmol) was added. The mixture was evaporated to dryness using vacuum to obtain a solid mixture and stirred continuously for six hours at room temperature. After the reaction, the solid mixture was extracted in dichloromethane solvent, filtered and dried in vacuum. The residue was then dissolved in dichloromethane and purified using a short column chromatography. Rapid elution with 15% ethylacetate:n-hexane solvent mixture afforded an orange colored compound, 1,1′-[CH(O)($\eta^5$-$C_5H_4$)Fe{($\eta^5$-$C_5H_4$) C(H)=NN(H)C(O)R}] {R = $C_6H_5$ (**3a**), $C_6H_4$–OH (**3b**)}. (Yield: **3a**: 162 mg (90%); **3b**: 173 mg (92%)).

**3a:** Anal. calcd. (found): C, 63.36 (63.51); H, 4.48 (4.57); N, 7.78 (7.64). IR($\nu$, $cm^{-1}$, $CH_2Cl_2$): 1678.5 (s), 1651 (vs), 1608 (s), 1557 (m). $^1$H NMR (δ, $CDCl_3$): 4.48 (s, 2H,

$\eta^5$-$C_5H_4$), 4.65 (t, 2H, $\eta^5$-$C_5H_4$), 4.87 (t, 4H, $\eta^5$-$C_5H_4$), 7.47–8.09 (m, 5H, -$C_6H_4$), 9.27 (s, 1H, -N*H*), 9.94 (s, 1H, -C*H*O). $^{13}$C NMR (δ, $CDCl_3$): 69.92 ($\eta^5$-$C_5H_4$), 70.88 ($\eta^5$-$C_5H_4$), 71.79 ($\eta^5$-$C_5H_4$), 74.35 ($\eta^5$-$C_5H_4$), 79.78 ($\eta^5$-$C_5H_4$), 79.81 ($\eta^5$-$C_5H_4$), 127.35 (Ar), 128.77 (Ar), 132.04 (Ar), 133.23 (Ar), 148.58 (-*C(H)*=), 164.03 (-*C*=O), 194.42 (-*C*=O). MS (ESI): m/z 362 $(M + 1)^+$.

**3b**: Anal. calcd. (found): C, 60.66 (60.79); H, 4.29 (4.16); N, 7.45 (7.52). IR(ν, $cm^{-1}$,$CH_2Cl_2$): 3394 (br), 3100 (br), 1681 (vs), 1656 (vs), 1607 (vs), 1491 (m), 1456 (m). $^1$H NMR (δ, $CDCl_3$): 4.50 (s, 2H, $\eta^5$-$C_5H_4$), 4.66 (s, 2H, $\eta^5$-$C_5H_4$), 4.89 (br, 4H, $\eta^5$-$C_5H_4$), 6.92–7.52 (m, 4H, -$C_6H_4$), 9.55 (s, 1H, -N*H*), 9.94 (s, 1H, -C*H*O), 11.92 (s, 1H, -O*H*). $^{13}$C NMR (δ, $CDCl_3$): 69.58 ($\eta^5$-$C_5H_4$), 71.01 ($\eta^5$-$C_5H_4$), 72.02 ($\eta^5$-$C_5H_4$), 74.45 ($\eta^5$-$C_5H_4$), 79.34 ($\eta^5$-$C_5H_4$), 79.69 ($\eta^5$-$C_5H_4$), 113.52 (Ar), 118.65 (Ar), 118.99 (Ar), 126.19 (Ar), 134.68 (Ar), 149.53 (Ar), 161.72 (-*C(H)*=), 166.29 (-*C*=O), 194.61 (-*C*=O).

## 3.4 | Synthesis of 1,1′-[{$(C_6H_5)C(CH_3)$=NN(H)C(O)C (CN)=CH}($\eta^5$-$C_5H_4$)Fe($\eta^5$-$C_5H_4$){CH=NN(H)C(O)$C_6H_5$}] (4)

(a) *Reaction of **3a** with [$(C_6H_5)C$ $(CH_3)$=NN(H)C(O)$CH_2CN$](**5**)*

Powdered Rice Husk Ash (RHA) (1gm) was taken in a two neck round bottomed flask and dichloromethane solution of **3a** (0.25 mmol, 90 mg) and 1 N-phenylethylidene-2-cyanoacetohydrazide (**5**) (0.25 mmol, 50 mg) was added. The mixture was evaporated to dryness to obtain a solid mixture and stirred continuously at 50 °C for eight hours. After the reaction, the solid mixture was extracted in dichloromethane solvent, filtered and dried in vacuum. The residue was then dissolved in dichloromethane and purification was done using a short column chromatography. Elution with 25% ethylacetate:n-hexane solvent mixture afforded a violet colored compound, 1,1′-[{$(C_6H_5)C$ $(CH_3)$=NN(H)C(O)C(CN)=CH}($\eta^5$-$C_5H_4$)Fe($\eta^5$-$C_5H_4$) {CH=NN(H)C(O)$C_6H_5$}] (***4***). (Yield: 113 mg (83%))

(b) *One pot three component reaction*

Dichloromethane solution of 1,1′- ferrocenyl carboxyladehyde (0.25 mmol, 61 mg), benzoic hydrazide (0.25 mmol, 34 mg) and **5** (0.25 mmol, 50 mg) was added to 1 gm of powdered Rice Husk Ash (RHA) in a two neck round bottomed flask. The mixture was evaporated to dryness to obtain a solid mixture and stirred initially for 4 hours at room temperature and then at 50 °C for eight hours. After the reaction, the solid mixture was extracted in dichloromethane solvent, filtered and dried in vacuum. The dried residue was dissolved in dichloromethane and purification was done using a short column chromatography. Elution with 25% ethylacetate:n-hexane solvent mixture afforded a violet colored compound, 1,1′-[{$(C_6H_5)C(CH_3)$=NN(H)C(O)C(CN)=CH}($\eta^5$-$C_5H_4$)Fe($\eta^5$-$C_5H_4$) {CH=NN(H)C(O)$C_6H_5$}] **(4)**. (Yield: 103 mg (76%)).

**4:** Anal. calcd. (found): C, 66.31 (66.47); H, 4.64 (4.57); N, 12.89 (12.77). IR(ν, $cm^{-1}$,$CH_2Cl_2$): 2210 (m), 1651 (vs), 1606 (m), 1581 (s), 1554 (m). $^1$H NMR (δ, $CDCl_3$): 2.31 (s, 3H, $CH_3$), 4.44 (s, 2H, $\eta^5$-$C_5H_4$), 4.79 (s, 2H, $\eta^5$-$C_5H_4$), 4.94 (s, 2H, $\eta^5$-$C_5H_4$), 5.13 (s, 2H, $\eta^5$-$C_5H_4$), 7.40–8.06 (m, 10H, -$C_6H_5$), 7.76 (s, 1H, -C*H*=), 8.16 (s, 1H, -C*H*=), 9.26 (s, 1H, NH), 9.78 (s, 1H, N*H*). $^{13}$C NMR (δ, $CDCl_3$): 29.71 (-$CH_3$), 70.29 ($\eta^5$-$C_5H_4$), 72.11 ($\eta^5$-$C_5H_4$), 72.60 ($\eta^5$-$C_5H_4$), 74.85 ($\eta^5$-$C_5H_4$), 76.14 ($\eta^5$-$C_5H_4$), 118.02 (Ar), 126.77 (Ar), 127.51 (Ar), 128.40 (Ar), 128.59 (Ar), 130.01 (Ar), 131.78 (Ar). MS (ESI): m/z 544 $(M + 1)^+$.

## 3.5 | Synthesis of [$(CN)CH_2C(O)N(H)N$=C$(CH_3)(Ar)$], {Ar = $C_6H_5$ (5), $C_9H_5O_2$ (6)}

In a two neck round bottomed flask, acetophenone (0.5 mmol, 0.06 ml) or 3-acetyl coumarin (0.5 mmol, 94 mg) and 2-cyanoacetohydrazide (0.5 mmol, 50 mg) was added to 1 gm of powdered Rice Husk Ash (RHA). The mixture was stirred continuously at 50 °C for eight hours. After the reaction, the solid mixture was extracted in dichloromethane solvent, filtered and dried in vacuum. The residue was then dissolved in dichloromethane and purification was done using column chromatography. Elution with 25% ethylacetate:n-hexane solvent mixture afforded a colorless compound, [(Ar)C $(CH_3)$ = NN(H) C(O)$CH_2CN$] {Ar = $C_6H_5$ (**5**), $C_9H_5O_2$ (**6**)}. (Yield: **5**: 92 mg (92%); **6**: 113 mg (84%)).

**5:** IR ($\nu_{CO}$, $cm^{-1}$, $CH_2Cl_2$): 2222 (m), 1693 (vs), 1640 (s), 1632 (m). $^1$H NMR (δ, $CDCl_3$): 2.29 (s, $CH_3$, 3H), 3.93(s, $CH_2$, 2H), 7.42–7.73(m, 5H), 9.23 (s, NH, 1H).

**6:** IR (ν, $cm^{-1}$,$CH_2Cl_2$): 2263 (m), 1727 (s), 1694 (vs), 1684 (s), 1607 (m). $^1$H NMR (δ, $CDCl_3$): 2.29 (s, 3H, $CH_3$), 3.83 (s, 2H, -C$H_2$-), 7.33–7.62 (m, 4H, -$C_9H_5O_2$), 8.07 (s, 1H, -$C_9H_5O_2$), 8.81 (s, 1H, N*H*).

*Spectral data of **5** and **6** has been matched with those previously reported.*[10]

## 3.6 | Synthesis of 1,1′-[HC(O)($\eta^5$-$C_5H_4$)Fe{($\eta^5$-$C_5H_4$)CH=C (CN)C(O)N(H)N=C$(CH_3)$R] {R = $C_6H_5$ (7), $C_9H_5O_2$ (8)}

(a) *One pot method*

Acetophenone (0.5 mmol, 0.06 ml) or 3-acetyl coumarin (0.5 mmol, 94 mg) and 2-cyanoacetohydrazide

(0.5 mmol, 50 mg) was added to 1 gm of powdered Rice Husk Ash (RHA) taken in a round bottom flask The mixture was stirred continuously at 50 °C temperature for eight hours. After the reaction, dichloromethane solution of 1,1′- ferrocenyl carboxaldehyde (0.5 mmol, 121 mg) was added. The solid mixture was dried and stirred continuously at room temperature for twelve hours. On completion of the reaction, the solid mixture was extracted in dichloromethane solvent, filtered and dried in vacuum. The residue was dissolved in dichloromethane and purification was done using a short column chromatography. Elution with 25% ethylacetate: n-hexane solvent mixture afforded a violet colored compound, 1,1′-[HC(O)($\eta^5$-$C_5H_4$)Fe{($\eta^5$-$C_5H_4$)CH=C (CN)C(O)N(H) N=C($CH_3$)R] {R = $C_6H_5$ (**7**), $C_9H_5O_2$ (**8**)}. (Yields: **7**: 174 mg (82%); **8**: 180 mg (73%)).

(b) *Reaction of Ferrocenyl dialdehyde with **5** or **6**.*

In a two neck round bottomed flask 1 gm of powdered Rice Husk Ash (RHA) was taken and dichloromethane solution of 1,1′- ferrocenyl carboxaldehyde (0.5 mmol, 121 mg) and **5** or **6** (0.5 mmol) was added. The mixture was evaporated to dryness to obtain a solid mixture and stirred continuously at room temperature for twelve hours. After the reaction, the solid mixture was extracted in dichloromethane solvent, filtered and dried in vacuum. The residue was then dissolved in dichloromethane and purification was done using a short column chromatography. Elution with 25% ethylacetate: n-hexane solvent mixture afforded a violet colored compound, 1,1′-[HC(O)($\eta^5$-$C_5H_4$)Fe{($\eta^5$-$C_5H_4$)CH=C(CN)C(O)N(H) N=C($CH_3$)R], {R = $C_6H_5$ (**7**), $C_9H_5O_2$ (**8**)}. (Yield: **7**: 183 mg (86%); **8**: 192 mg (78%))

**7:** Anal. calcd. (found): C, 64.96 (65.12); H, 4.50 (4.41); N, 9.88 (9.97). IR ($\nu$, $cm^{-1}$,$CH_2Cl_2$): 2214 (m), 1682 (vs), 1663(vs), 1589 (s), 1527 (m), 1455 (m). $^1$H NMR (δ, $CDCl_3$):

**TABLE 5** Crystal data and structure refinement parameters for compounds **1a** and **2**

| | **1a** | **2** |
|---|---|---|
| Empirical formula | $C_{21}H_{20}FeN_2O_2$ | $C_{17}H_{17}FeN_3O_2$ |
| Formula weight | 388.24 | 351.18 |
| Crystal system | Orthorhombic | Monoclinic |
| Space group | Pca21 | $P2_1/n$ |
| *a*, Å | 8.6622(9) | 8.8762(2) |
| *b*, Å | 9.6048(9) | 22.3127(6) |
| *c*, Å | 41.472(4) | 15.3692(5) |
| $\alpha$ deg | 90° | 90° |
| $\beta$ deg | $90^0$ | 95.582(2)° |
| $\gamma$ deg | 90° | 90° |
| V, $Å^3$ | 3450.5(6) | 3029.47(15) |
| Z | 8 | 8 |
| Dcalcd, Mg $m^{-3}$ | 1.495 | 1.540 |
| abs coeff, $mm^{-1}$ | 0.892 | 1.009 |
| F(000) | 1616 | 1456 |
| Cryst size, mm | 0.208 x 0.207 x 0.070 | 0.170 x 0.030 x 0.020 |
| θ range, deg | 2.892° to 30.482° | 1.825 to 26.000° |
| index ranges | −12 < =h < =9, −13 < =k < =13, −58 < =l < =58 | −10 < =h < =10, −27 < =k < =27, −18 < =l < =18 |
| reflections collected/unique | 60946/10004 [R (int) = 0.0337] | 53105/5627 [R (int) = 0.1158] |
| data/restraints/parameters | 10004/471/460 | 5627/0/419 |
| goodness-of-fit on $F^2$ | 1.087 | 1.080 |
| Final R indices [$I > 2\sigma(I)$] | R1 = 0.0442, wR2 = 0.1127 | R1 = 0.0467, wR2 = 0.0738 |
| R indices (all data) | R1 = 0.0517, wR2 = 0.1253 | R1 = 0.0988, wR2 = 0.0953 |
| largest diff peak | 1.835 | 0.476 |
| and hole, $eÅ^{-3}$ | −0.623 | −0.478 |

2.42 (s, 3H, $CH_3$), 4.69 (s, 2H, $\eta^5$-$C_5H_4$), 4.79 (s, 2H, $\eta^5$-$C_5H_4$), 4.90 (s, 2H, $\eta^5$-$C_5H_4$), 5.12 (s, 2H, $\eta^5$-$C_5H_4$), 7.44–7.89 (m, 4H, -$C_6H_5$), 8.26 (s, 1H, -C*H*=), 9.26 (br, 1H, NH), 9.91 (s, 1H, -C*H*O). $^{13}$C NMR (δ, $CDCl_3$): 13.34 (-*C*$H_3$), 71.37 ($\eta^5$-*C*$_5H_4$), 72.37 ($\eta^5$-*C*$_5H_4$), 72.52 ($\eta^5$-*C*$_5H_4$), 74.64 ($\eta^5$-*C*$_5H_4$), 74.79 ($\eta^5$-*C*$_5H_4$), 80.93 ($\eta^5$-*C*$_5H_4$), 126.29 (Ar), 126.86 (Ar), 128.54 (Ar), 130.00 (Ar), 130.36 (-*C*H=), 137.33 (-*C*H=), 154.33 (-*C*N), 154.84 (-*C*=O), 192.31 (-*C*=O). MS (ESI): m/z 426.9 $(M + 1)^+$.

**8:** Anal. calcd. (found): C, 63.31 (63.47); H, 3.88 (3.72); N, 8.52 (8.64). IR (ν, $cm^{-1}$,$CH_2Cl_2$): 2214 (m), 1730 (vs), 1714 (vs), 1682 (vs), 1607 (s), 1494 (s), 1456 (s). $^1$H NMR (δ, $CDCl_3$): 2.43 (s, 3H, $CH_3$), 4.68 (s, 2H, $\eta^5$-$C_5H_4$), 4.79 (s, 2H, $\eta^5$-$C_5H_4$), 4.89 (s, 2H, $\eta^5$-$C_5H_4$), 5.11 (s, 2H, $\eta^5$-$C_5H_4$), 7.32–8.23 (m, 5H, $C_9H_5O_2$), 8.24 (s, 1H, -C*H*=), 9.36 (s, 1H, NH), 9.89 (s, 1H, -C*H*O). MS (ESI): m/z 494.11 $(M + 1)^+$.

## 3.7 | Computational details

Geometry optimization of compound **2** in different conformers were carried out by using density functional theory (DFT) at B3LYP and M06-2X level of theory using LANL2DZ basis sets.[15,16] In addition to optimization, energy calculation in gas and solution phase was carried out at the same level of basis sets. The natural frontier molecular orbitals (FMO) have been analyzed.

## 3.8 | Antibacterial activity

Compounds **2, 3a, 3b, 4, 7** and **8** were screened for their antibacterial activity in vitro following the protocol described elsewhere.[17] The antibacterial effect was assayed against both Gram positive bacteria *Bacillus subtilis* and Gram negative bacteria, *Escherichia coli* and *Pseudomonas aeruginosa* and *Vibrio cholarae* by the agar well diffusion method.[17] The compound was dissolved in 2% DMSO at different concentrations ranging from 62.5 to 1.0 μg/ml. Mueller Hinton-agar (containing 1% peptone, 0.6% yeast extract, 0.5% beef extract and 0.5% NaCl, at pH 6.9–7.1) plates were prepared and 0.5 – McFarland culture (1.5 X $10^8$ cells/ml) of the test organisms were swabbed onto the agar plate. 9 mm wells were made in the LB agar petri dishes. 100 μl of each of the compound with decreasing concentrations was added to separate wells. DMSO was used as the negative control and Ampicillin and Vancomycin was taken as positive control. The plates were incubated at 37 °C and observed for zones of inhibition around each well after 24 hrs. The MIC, defined as the lowest concentration of the test compound, which inhibits the visible growth, was determined visually after incubation for 24 hr at 37 °C.

## 3.9 | Crystal structure determination for 1a and 2

Single crystal X-ray structural studies of **1a** and **2** were performed on a CCD Oxford Diffraction XCALIBUR-S diffractometer equipped with an Oxford Instruments low-temperature attachment. Data were collected at 150(2) K using graphite-monochromated Mo Kα radiation ($\lambda_\alpha$ = 0.71073 Å). The strategy for the data collection was evaluated by using the CrysAlisPro CCD software. The data were collected by the standard 'phi-omega scan techniques, and were scaled and reduced using CrysAlisPro RED software. The structures were solved by direct methods using SHELXS-97 and refined by full matrix least-squares with SHELXL-97, refining on $F^2$.[18] The positions of all the atoms were obtained by direct methods. All non-hydrogen atoms were refined anisotropically. The crystallographic details are summarized in Table 5.

## ACKNOWLEDGEMENTS

S.C. is grateful to the Department of Science and Technology (SERB), Government of India, for research funding (No. SB/S1/IC-30/2013). We are thankful to Soliel Oilex Pvt Ltd, WB, India, for providing us with Rice Husk and Rice Hush ash for the reaction purposes.

## ORCID

*Shaikh M. Mobin* https://orcid.org/0000-0003-1940-3822
*Saurav Chatterjee* https://orcid.org/0000-0002-6290-4342

## REFERENCES

[1] (a) K. Tanaka, F. Toda, *Chem. Rev.* **2000**, *100*, 1025. (b) H. Zhu, S. Ould-Chikh, H. Dong, I. Llorens, Y. Saih, D. H. Anjum, J. L. Hazemann, J. M. Basset, *ChemCatChem* **2015**, *7*, 3332. (c) J. Cleophax, M. Liagre, A. Loupy, A. Petit, *Org. Process Res. Dev.* **2000**, *4*, 498. (d) F. Toda, *Acc. Chem. Res.* **1995**, *28*, 480. (e) G. W. V. Cave, C. L. Raston, J. L. Scott, *Chem. Commun.* **2001**, 2159. (f) T. W. Elkins, H. E. Hagelin-Weaver, *Appl. Catal., A* **2015**, *497*, 96. (g) J. Xu, R. D. Armstrong, G. Shaw, N. F. Dummer, S. J. Freakley, S. H. Taylor, G. J. Hutchings, *Catal. Today* **2016**, *270*, 93.

[2] (a) J. T. Grant, J. M. Venegas, W. P. McDermott, I. Hermans, *Chem. Rev.* **2018**, *118*, 2769. (b) K. Tanaka, *Solvent-free Organic Synthesis*, Wiley-VCH, Weinheim **2003**. (c) J. G. Hernández, E. Juaristi, *J. Org. Chem.* **2010**, *75*, 7107. (d) A. Rahman, S. B. Jonnalagadda, *Catal. Lett.* **2008**, *123*, 264. (e) K. R. Kloetstra, H. V. Bekkum, *Chem. Commun.* **1995**, *0*, 1005. (f) B. M. Choudary, M. L. Kantam, A. Rahman, C. V. R. Reddy, *J. Mol. Catal.* **2003**, *206*, 145. (g) S. Wada, H. Suzuki, *Tetrahedron Lett.* **2003**, *44* 399. (h) S. M. Roberts (Ed), *Catalysts for fine chemicals*

*synthesis, Microporous and Mesoporous Solid Catalysts*, Vol. 4, Wiley-VCH, New York, **2006**.

[3] (a) P. Serna, B. C. Gates, *Acc. Chem. Res.* **2014**, *47*, 2612. (b) D. Hellwinkel, K. Göke, *Synthesis* **1995**, *1995*, 1135. (c) M. R. Detty, R. S. Eachus, J. A. Sinicropi, J. R. Lenhard, M. McMillan, A. M. Lauzafame, H. R. Luss, R. Young, J. E. Eilers, *J. Org. Chem.* **1995**, *60*, 1674. (d) E. Stankovic, S. Toma, R. V. Boxel, I. Asselberghs, A. Persoons, *J. Organomet. Chem.* **2001**, *637*, 426. (e) D. Villemin, A. BenAlloum, *Phosphorus Sulfur Silicon* **1993**, *79*, 33. (f) G. Cooke, H. M. Palmer, O. Schulz, *Synthesis* **1995**, *1995*, 1415. (g) E. Stankovic, P. Elecko, S. Toma, *Chem. Pap.* **1996**, *50*, 68. (h) G. Cooke, O. Schulz, *Synth. Commun.* **1996**, *26*, 2549.

[4] (a) M. Patra, G. Gasser, *ChemBioChem* **2012**, *13*, 1232. (b) G. Gasser, N. Metzler-Nolte, *Curr. Opin. Chem. Biol.* **2012**, *16*, 84. (c) E. Meggers, G. E. A. Gokcumen, H. Bregman, J. Maksimoska, S. P. Mulcahy, N. Pagano, D. S. Williams, *Synlett* **2007**, *2007*, 1177. (d) C. Policar, J. B. Waern, M.-A. Plamont, S. Clède, C. Mayet, R. Prazeres, J.-M. Ortega, A. Vessières, A. Dazzi, *Angew. Chem. Int. Ed.* **2011**, *50*, 860. (e) C. G. Hartinger, N. Metzler-Nolte, P. J. Dyson, *Organometallics* **2012**, *31*, 5677. (f) C. G. Hartinger, P. J. Dyson, *Chem. Soc. Rev.* **2009**, *38*, 391. (g) R. H. Fish, G. Jaouen, *Organometallics* **2003**, *22*, 2166. (h) S. Top, A. Vessières, C. Cabestaing, I. Laios, G. Leclercq, C. Provot, G. Jaouen, *J. Organomet. Chem.* **2001**, *637*, 500. (i) A. Nguyen, A. Vessières, E. A. Hillard, S. Top, P. Pigeon, G. Jaouen, *Chimia* **2007**, *61*, 716. (j) E. A. Hillard, P. Pigeon, A. Vessieres, C. Amatore, G. Jaouen, *Dalton Trans.* **2007**, *0*, 5073. (k) E. A. Hillard, A. Vessières, L. Thouin, G. Jaouen, C. Amatore, *Angew. Chem. Int. Ed.* **2006**, *45*, 285. (l) M. Patra, G. Gasser, N. Metzler-Nolte, *Dalton Trans.* **2012**, *41*, 6350. (m) E. I. Edwards, R. Epton, G. Marr, *J. Organomet. Chem.* **1975**, *85*, C23. (n) E. I. Edwards, R. Epton, G. Marr, *J. Organomet. Chem.* **1976**, *107*, 351. (o) J. T. Chantson, M. V. V. Falzacappa, S. Crovella, N. Metzler-Nolte, *J. Organomet. Chem.* **2005**, *690*, 4564. (p) M. Patra, G. Gasser, A. Pinto, K. Merz, I. Ott, J. E. Bandow, N. Metzler-Nolte, *ChemMedChem* **2009**, *4*, 1930. (q) M. Patra, G. Gasser, M. Wenzel, K. Merz, J. E. Bandow, N. Metzler-Nolte, *Organometallics* **2012**, *31*, 5760. (r) M. Patra, K. Merz, N. Metzler-Nolte, *Dalton Trans.* **2012**, *41*, 112.

[5] (a) S. Mishra, S. Dewangan, S. Giri, S. M. Mobin, S. Chatterjee, *Eur. J. Inorg. Chem.* **2016**, *2016*, 5485. (b) V. Tirkey, S. Mishra, H. R. Dash, S. Das, B. P. Nayak, S. M. Mobin, S. Chatterjee, *J. Organomet. Chem.* **2013**, *732*, 122. (c) S. K. Patel, V. Tirkey, S. Mishra, H. R. Dash, S. Das, M. Shukla, S. Saha, S. M. Mobin, S. Chatterjee, *J. Organomet. Chem.* **2014**, *749*, 75. (d) S. Mishra, V. Tirkey, A. Ghosh, H. R. Dash, S. Das, M. Shukla, S. Saha, S. M. Mobin, S. Chatterjee, *J. Mol. Struct.* **2015**, *1085*, 162. (e) V. Tirkey, R. Boddhula, S. Mishra, S. M. Mobin, S. Chatterjee, *J. Organomet. Chem.* **2015**, *794*, 88. (f) A. Ghosh, S. Mishra, S. Giri, S. M. Mobin, A. Bera, S. Chatterjee, *Organometallics* **2018**, *37*, 1999. (g) R. Boddhula, A. Ghosh, C. Wölper, S. M. Mobin, S. Giri, S. Chatterjee, *J. Organomet. Chem.* **2017**, *851*, 22.

[6] (a) H. Miyaji, S. R. Collinson, I. J. Prokes, H. R. Tucker, *Chem. Commun.* **2003**, *0*, 64; (b) D. Mandal, P. Deb, B. Mondal, A. Thakur, S. J. Ponniah, S. Ghosh, *RSC Adv.* **2013**, *3*, 18614. (c) T. Kienz, C. Förster, K. Heinze, *Organometallics* **2014**, *33*, 4803. (d) J. M. Speck, M. Korb, T. Rüffer, A. Hildebrandt, H. Lang, *Organometallics* **2014**, *33*, 4813. (e) A. K. Diallo, C. Absalon, J. Ruiz, D. Astruc, *J. Am. Chem. Soc.* **2011**, *133*, 629. (f) F. Strehler, M. Korb, E. A. Poppitz, H. Lang, *J. Organomet. Chem.* **2015**, *786*, 1. (g) F. Otón, M. C. González, A. Espinosa, C. R. Arellano, A. Tárraga, P. Molina, *J. Org. Chem.* **2012**, *77*, 10083. (h) R. Deng, Y. Huang, X. Ma, G. Li, R. Zhu, B. Wang, Y.-B. Kang, Z. Gu, *J. Am. Chem. Soc.* **2014**, *136*, 4472.

[7] (a) W.-Y. Liu, Q.-H. Xu, B.-H. Chen, Y.-M. Liang, Y.-X. Ma, W.-M. Liu, *J. Organomet. Chem.* **2001**, *637*, 782. (b) J. A. Mata, E. Peris, *J. Chem. Soc. Dalton Trans.* **2001**, 3634. (c) C. Manzur, L. Millán, M. Fuentealba, J. A. Mata, D. Carrillo, J.-R. Hamon, *J. Organomet. Chem.* **2005**, *690*, 1265. (d) V. B. Golovko, M. J. Mays, G. A. Solan, *J. Organomet. Chem.* **2008**, *693*, 2683.

[8] (a) J. James, M. SubbaRao, *Am. Ceram. Soc. Bull.* **1986**, *65*, 1177. (b) S. Chandrasekhar, P. N. Pramada, P. Raghavan, K. G. Satyanarayana, T. N. Gupta, *J. Mater. Sci. Lett.* **2002**, *21*, 1245. (c) S. Chandrasekhar, P. N. Pramada, J. Majeed, *J. Mater. Sci.* **2006**, *41*, 7926.

[9] (a) F. Adam, J. N. Appaturi, A. Iqbal, *Catal. Today* **2012**, *190*, 2. (b) S. Cui, S.-W. Yu, B.-L. Lin, X.-D. Shen, D. Gu, *RSC Adv.* **2015**, *5*, 65818. (c) S. K. Rajanna, D. Kumar, M. Vinjamur, M. Mukhopadhyay, *Ind. Eng. Chem. Res.* **2015**, *54*, 949. (d) A. Tadjarodi, M. Haghverdi, V. Mohammadi, *Mater. Res. Bull.* **2012**, *47*, 2584. (e) F.-W. Chang, T.-J. Hsiao, J.-D. Shih, *Ind. Eng. Chem. Res.* **1998**, *37*, 3838. (f) L. Wang, Z. Schnepp, M. M. Titirici, *J. Mater. Chem. A* **2013**, *1*, 5269. (g) S. Kumagai, M. Sato, D. Tashim, *Electrochim. Acta* **2013**, *114*, 617. (h) L. M. Ombaka, P. G. Ndungu, B. Omondi, V. O. Nyamori, *J. Coord. Chem.* **2014**, *67*, 1905.

[10] (a) K. N. Zelenin, S. V. Oleinik, V. V. Alekseev, A. A. Potekhin, *Russ. J. Gen. Chem.* **2001**, *71*, 1116. (b) S. M. Gomha, K. D. Khalil, *Molecules* **2012**, *17*, 9335.

[11] (a) T. Moriuchi, T. Hirao, *Top Organomet. Chem.* **2006**, *17*, 143. (b) T. Moriuchi, K. Yoshida, T. Hirao, *Organometallics* **2001**, *20*, 3101. (c) T. Moriuchi, T. Nagai, T. Hirao, *Org. Lett.* **2005**, *7*, 5265. (d) W. Bauer, K. Polborn, W. Beck, *J. Organomet. Chem.* **1999**, *579*, 269.

[12] U. T. Mueller-Westerhoff, Z. Yang, G. Ingram, *J. Organomet. Chem.* **1993**, *463*, 163.

[13] M. Vogel, M. Rausch, H. Rosenberg, *J. Org. Chem.* **1957**, *22*, 1016.

[14] (a) N. S. Navaneetham, R. Kalyanasundaram, S. Soundararajan, *Inorg. Chim. Acta* **1985**, *110*, 169. (b) H. Meyer, J. Mally, *Monatsh. Chem.* **1912**, *33*, 393. (c) P. Singh, R. Kumar, B. K. Yadav, R. S. Khanna, A. K. Tewari, *RSC Adv.* **2014**, *4*, 51239.

[15] A. D. Becke, *J. Chem. Phys.* **1993**, *98*, 5648.

[16] C. Lee, W. Yang, R. G. Parr, *Phys. Rev. B* **1988**, *37*, 785.

[17] (a) Clinical and Laboratory Standards Institute (CLSI, 2006), *Methods for Dilution Antimicrobial Susceptibility Tests for Bacteria That Grow Aerobically*, Seventh ed. *Approved Standard M7-A7*, CLSI, Wayne, PA, USA, **2006**. (b) A. U. Rahman, M. I. Choudhary, W. J. Thomsen, *Bioassay techniques for drug development*, Harwood Academic Publishers, The Netherlands, **2001**, 22.

[18] (a) G. M. Sheldrick, *SHELXL*-2014*, Program for the Refinement of Crystal Structures, University of Göttingen, Göttingen (Germany)*, **2014**; (b) G. M. Sheldrick, *Acta Crystallogr., Sect. A: Fundam. Crystallogr.* **2008**, *64*, 112.

## SUPPORTING INFORMATION

Additional supporting information may be found online in the Supporting Information section at the end of the article.

**How to cite this article:** Ghosh A, Barik T, Dewangan S, et al. Selective functionalization of ferrocenyl compounds using a novel solvent free synthetic method for the preparation of bioactive unsymmetrical ferrocenyl derivatives. *Appl Organometal Chem*. 2019;e4838. https://doi.org/10.1002/aoc.4838